Theoretical and Applied Climatology (2020) 139:773–784
https://doi.org/10.1007/s00704-019-03010-8

ORIGINAL PAPER

Land surface temperature variability across India: a remote sensing satellite perspective

Satya Prakash [1] · Hamid Norouzi [2,3]

Received: 17 July 2019 / Accepted: 16 September 2019 / Published online: 4 November 2019

Abstract

Land surface temperature (LST) plays a key role in the surface energy budget computation and land surface process studies. The Moderate Resolution Imaging Spectroradiometer (MODIS) sensors onboard the Aqua and Terra satellites provide comprehensive global LST estimates at a fine spatial resolution. The MODIS products were recently upgraded to Collection 6, and shown to be more accurate than its predecessor Collection 5 products. In this study, LST and its variability have been examined across India from Collection 6 of the Aqua MODIS data at 0.05° spatial resolution for the period of 2003 to 2017. All-India mean LST characteristics show distinctive features as compared to the well-documented mean characteristics of near-surface air temperature. All land cover types except permanent snow and ice, and cold desert areas exhibit bimodal peaks in seasonal variations of daytime LST. The daytime LST over the coldest and high-altitude regions of northern India shows anomalous positive linear relationship with NDVI at a monthly scale. However, monthly domain-mean daytime LST of cropland regions is largely negatively correlated with NDVI as compared to other land cover types. Results reveal that about 17% of the Indian landmass received its hottest LST during 2010 followed by 2016. Linear trend analysis for the 15-year period of mean annual LST shows a decrease in diurnal temperature range over most parts of the country due to rather rapid increase in nighttime LST than daytime LST, similar as changes in near-surface air temperature across the country.

1 Introduction

Land surface temperature (LST), also known as land skin temperature, is one of the crucial parameters for the study of surface energy budget, land surface processes, urban heat islands, and for the retrieval of several atmospheric variables (Li et al. 2013; Norouzi et al. 2015a; Didari et al. 2017; Deilami et al. 2018; Prakash et al. 2018; Susskind et al. 2019). LST also plays a key role in the land surface model data assimilation. LST of a specific location is generally controlled by the surface air temperature along with other surface and sub-surface parameters such as soil moisture, soil roughness, vegetation type, elevation, shortwave, and longwave radiations. Although surface air temperature and LST are locally correlated, the magnitudes of their diurnal variations have notable differences (Prakash et al. 2019). The response of LST to changes in local energy balance is faster than the surface air temperature. An adequate knowledge of differences among LST, surface air temperature, and upper layer soil temperature is vital for several environmental applications (Prakash et al. 2017; Shati et al. 2018).

Ground-based observations of LST are rather sparse and limited at the global scale, and remote sensing satellites provide a cost-effective alternative to measure global and regional LST comprehensively. LST measurements from the polar-orbiting satellites are generally used as reference for validating LST derived from the geostationary satellites over in-situ data sparse regions (Singh et al. 2016). LST estimates from the Moderate Resolution Imaging Spectroradiometer (MODIS) sensors onboard the polar-orbiting Aqua and Terra satellites have been widely used for various applications at global and regional scales (Li et al. 2013; Prakash et al. 2016, 2018; Deilami et al. 2018; Phan and Kappas 2018; Sharifnezhadazizi et al. 2019). MODIS-derived LST estimates were also utilized to assess short-term changes in LST over India at local scale (Mathew et al. 2017; Patel

✉ Satya Prakash
sprakash012@gmail.com

[1] Divecha Centre for Climate Change, Indian Institute of Science, Bengaluru 560012, India

[2] New York City College of Technology, City University of New York, Brooklyn, NY 11201, USA

[3] Earth and Environmental Sciences, The Graduate Center, City University of New York, New York, NY 10016, USA

et al. 2017). Furthermore, these LST estimates were used to identify the hottest spot on the Earth located in the southeast Iran and its variations during MODIS-era (Mildrexler et al. 2011). Even though infrared-based LST estimates are more accurate and available at finer spatial resolution than those from passive microwave sensors, infrared-based LST estimates are available for clear-sky conditions alone. Hence, the synergism of infrared and passive microwave estimates of LST using a suitable technique has been advocated to achieve comprehensive global estimates of all-weather LST (Li et al. 2013; Prigent et al. 2016).

Elevation and normalized difference vegetation index (NDVI) have shown to be closely related with the maximum LST (Khandan et al. 2018). Nonetheless, the changes in LST are also controlled by the vegetation types (Parida et al. 2008; Mildrexler et al. 2011). A negative linear relationship between LST and NDVI, and a positive correlation between LST and elevation was found over an urban area of the western India (Mathew et al. 2017). In general, LST is positively correlated with NDVI over the higher latitudes and elevations where energy is the limiting factor for vegetation growth, whereas there is a negative correlation between LST and NDVI over the regions where water is the limiting factor for vegetation growth (Karnieli et al. 2010). Moreover, the strength of correlations between LST and NDVI primarily depends on the season and land cover type (Marzban et al. 2018).

In the global climate change context, substantial changes in surface air temperature and precipitation extremes from the second half of twentieth century at global and regional scales have been reported using observations and climate models (Hao et al. 2013; Schmidt et al. 2014; Turco et al. 2015). Near-surface warming has been found to be the largest over desert regions, resulting in desert amplification due to combined effect of warming and moistening of the troposphere (Wei et al. 2017). As annual maximum LST estimates are capable to characterize the changes in land cover and extreme climate events such as droughts and heat waves (Mildrexler et al. 2018), a comprehensive assessment of the variability in annual maximum LST at regional scale is vital for socio-economic benefits. Using daytime LST Collection 5 data from the Aqua MODIS sensor for 2003–2014, Mildrexler et al. (2018) showed large-scale directional shifts in the global maximum LST that indicated change in the surface energy balance. A significant warming of LST (~0.28 K decade^{-1}) between 2003 and 2013 was evident due to deforestation over the tropical regions (Li et al. 2016). Recently, Zhao et al. (2019) utilized LST products from the MODIS sensors to assess the trends in mean annual LST and annual maximum LST over the central Himalayan region, and reported that these two parameters are increasing at a faster rate during daytime than nighttime. A considerable decrease in forest cover in central and northeast India, and growth of cropland area in western India were also noticed between 1985 and 2005 using satellite-derived decadal land use/land cover data (Roy et al. 2015).

Recently, MODIS products have gone through major improvements and Collection 6 products were released. The Collection 6 of MODIS products were proven to be more accurate than their predecessor Collections (Wan 2014; Duan et al. 2019). As India is one of the largest countries in the world and comprises of varied topography and land cover (e.g., Fig. 1), it becomes imperative to assess the variations in LST across the country for several environmental applications and policy planning. The ground observations of LST across the country are very sparse and generally not accessible publicly. The objective of this study is to comprehensively assess the variations in LST across India from the Aqua MODIS product for a 15-year period spanning from 2003 to 2017.

2 Data used

The MODIS sensors, mounted at two polar-orbiting satellites—Aqua and Terra, measure atmospheric, oceanic, and land surface parameters at fine spatial resolution. MODIS sensors have 36 visible and infrared channels which operate between the spectral ranges of 0.4 μm and 14.4 μm (Justice et al. 1998). The equatorial crossing local times of the Terra satellite are about 10:30 and 22:30, whereas these are 01:30 and 13:30 for the Aqua satellite. As LST observations around 13:30 local time are closer to the daily maximum LST of a given location (Sharifnezhadazizi et al. 2019), LST observations from the Aqua MODIS were used in this study. The Aqua satellite, with six sensors onboard, was launched on May 4, 2002 by the National Aeronautics and Space Administration (NASA) with a goal to better understand the global water and energy budget (Parkinson 2013). This satellite was the first member of the Afternoon Constellation or A-Train.

The cloud-free daily LST product—MYD11C1 Collection 6 (Wan et al. 2015) for January 2003 to December 2017 has been considered in this study. Collection 6 LST products showed notable differences from Collection 5 products, particularly over the global arid regions (Prakash et al. 2018). The accuracy of Collection 6 LST products was shown to be better than that of Collection 5 products due to substantial improvement in the retrieval algorithms (Wan 2014; Duan et al. 2019). Monthly Aqua MODIS NDVI dataset—MYD13C2 Collection 6 (Didan 2015) and annual land cover dataset from the combined Terra and Aqua MODIS—MCD12C1 Collection 6 (Friedl and Sulla-Menashe 2015) for the 15-year period were also used in this study. Collection 6 land cover products have shown to be more accurate than Collection 5 due to refinements in the algorithm (Sulla-Menashe et al. 2019). These three MODIS-derived products are available globally at 0.05° (~5.6 km at the equator)

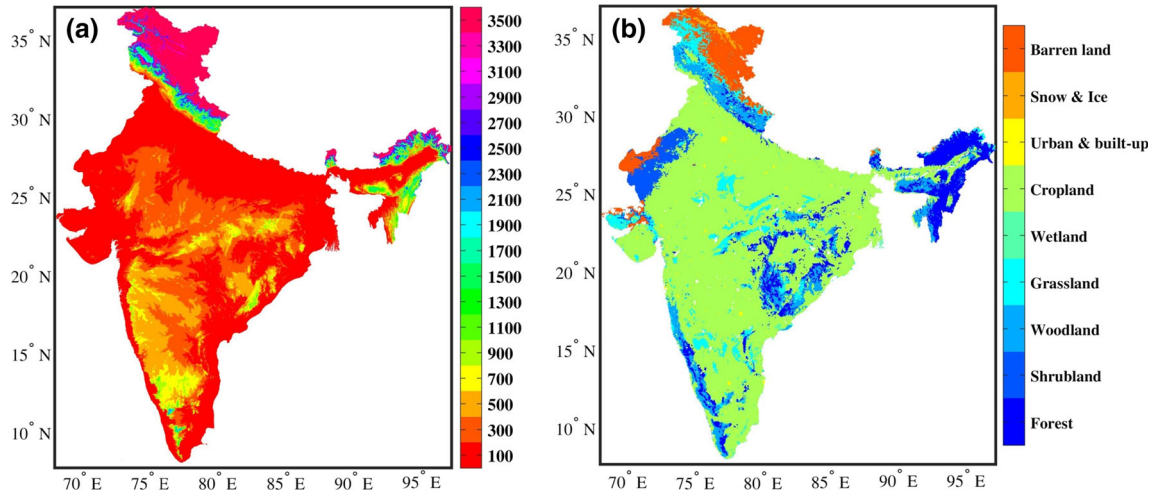

Fig. 1 Spatial distributions of **a** GTOPO30 topography (m) and **b** MODIS land cover types for 2017 across India

climate modeling grid. MODIS-derived LST and NDVI products along with precipitation and soil moisture datasets were already shown to be promising for drought monitoring across India (Prakash 2018).

Monthly cloud cover product from the Aqua MODIS (Platnick et al. 2015) for 2003 to 2017 was also used. Additionally, GTOPO30 dataset (Gesch and Larson 1996) was used to characterize the distinct topographical features across India. GTOPO30 is a global digital elevation model produced by the United States Geological Survey (USGS) with a horizontal grid spacing of 30 arc seconds (~ 1 km at the equator).

3 Results and discussion

3.1 Topography and land cover across India

Figure 1a shows the spatial distributions of topography across India using GTOPO30 dataset. It can be seen that the country comprises of highly varied topographical features. The northern parts of India have high mountains with elevation greater than 3 km (e.g., the Himalayan mountain range), whereas the western India and the Himalayan foothills regions have elevation less than 300 m. The southern and central parts of India have elevations ranging from 100 m to about 1 km due to existence of several mountain ranges, valleys, and plateaus. The northeast India itself showed a wide variation in elevation such as high elevation in northern and southern parts, and lower elevation in central parts. Such diverse topographical characteristics along with unique geography lead to distinct weather patterns with large spatio-temporal variability across the country.

The spatial distributions of MODIS land cover across India for the year 2017 are presented in Fig. 1b. The MODIS land covers were divided into 17 classes according to the International Geosphere-Biosphere Programme (IGBP). The first IGBP class of water bodies is not considered in this study, and remaining 16 IGBP classes were further grouped into 9 land cover classes. Five IGBP land cover classes such as evergreen needleaf forests, evergreen broadleaf forests, deciduous needleaf forests, deciduous broadleaf forests, and mixed forests were categorized as one land cover class namely, forest. Closed shrublands and open shrublands were grouped as shrubland, while woody savannas, and savannas were classified as woodland. Similarly, croplands, and cropland/natural vegetation mosaics were grouped as cropland. Cropland covered about 64% of land area across the country. About 9% of land area was covered by forests, whereas woodland and grassland occupied about 16% of land area altogether. Permanent wetlands, and permanent snow and ice covered less than 1% of the Indian land area. All these nine land cover types exhibit considerable interannual variations between 2003 and 2017. A considerable increase in cropland and urban areas, and a significant decrease in forests and wasteland between 1985 and 2005 over India were reported using multispectral decadal satellite data (Roy et al. 2015). Although barren land covers 7% of land area across India, they are indeed of two types. The barren land over the western parts of India comes under the range of Thar desert and known as "hot desert," whereas the barren land over the northern parts of India are known as "cold desert." These two types of barren land have essentially distinct impacts on land surface processes. Hence, barren land areas were further classified into two groups for subsequent analyses.

3.2 Mean characteristics of LST across India

Figure 2 presents the spatial distributions of 15-year mean monthly daytime and nighttime LST across India from the Aqua MODIS product. Highest elevation regions of northern

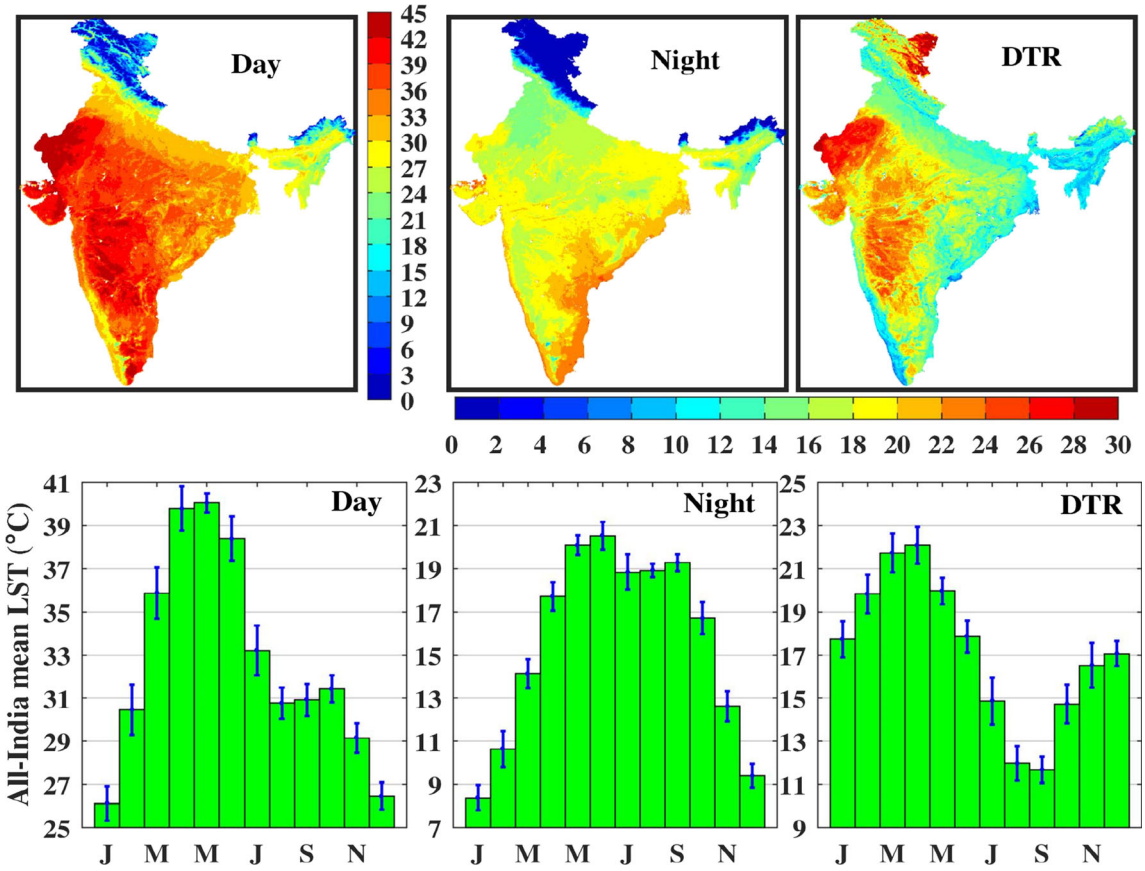

Fig. 2 (Upper panel) Spatial distributions of mean land surface temperature (°C), and (lower panel) monthly variations in all-India mean land surface temperature for daytime and nighttime and their differences for the period 2003–2017. The error bars present interannual variations

India and northern parts of northeast India show the smallest mean LST during both daytime and nighttime. As expected, highest mean daytime LST of more than 44 °C can be seen over the desert region of western India. However, the southeastern coastal regions exhibit the warmest mean LST during nighttime. In general, southern India shows larger mean LST than northern India. The regions of elevation between 500 and 900 m in the southern India exhibit higher mean daytime LST than its surroundings. The difference between daytime and nighttime LST, termed as diurnal temperature range (DTR), shows rather smaller magnitude (< 12 °C) along the southwest coast, northeast India, and over the Himalayan foothills. The barren land and shrubland regions of western and northern India show DTR as high as 25 °C.

The monthly variations of all-India mean LST for the 15-year period are also presented in Fig. 2. Daytime LST shows its peak during the month of May with rather smaller interannual variability. April is the second hottest month followed by June. However, June is the hottest month followed by May as far as nighttime LST is concerned. January is the coolest month followed by December for both daytime and nighttime LST. All-India DTR is shown to be largest during the month of April followed by March. The smallest DTR exhibits during August and September. Bimodal characteristics of all-India LST can also be seen for these three estimates (e.g., daytime, nighttime, and DTR). These mean features of LST over India reveal that the characteristics of LST are not exactly same as the mean characteristics of near-surface air temperature. For instance, all-India mean DTR of near-surface air temperature shows the maximum during March and minimum during July and August. These results also support the fact that there are considerable differences between LST and near-surface air temperature variability as reported for other parts of the globe (e.g., Prakash et al. 2019).

As daytime LST is closely related to the land cover and NDVI (Parida et al. 2008; Mildrexler et al. 2011; Khandan et al. 2018), the seasonal cycle of domain-mean daytime LST for different land cover types are illustrated in Fig. 3. Except permanent snow and ice and cold desert areas, all land cover types exhibit bimodal peak in mean LST. The first peak in mean LST with largest magnitude associated with the northern hemispheric summer season can be observed during April for shrubland, cropland, urban, and hot deserts, while it is May for forest, woodland, grassland, and permanent wetland. The mean LST reaches up to 50 °C during April and May for hot desert and shrubland. The secondary peak in mean LST is observed during the month of October, after withdrawal of

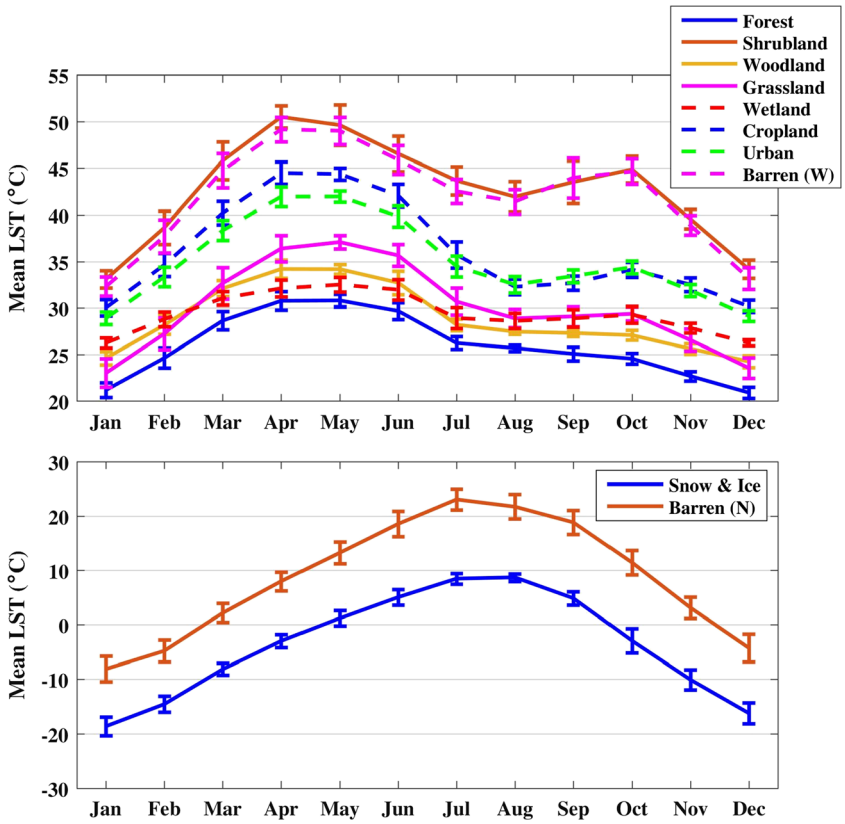

Fig. 3 Monthly variations in domain-mean daytime land surface temperature (2003–2017) over India for different land cover types. The error bars present interannual variations

the southwest monsoon season. However, the secondary peak is found to be rather weaker for forest, woodland, grassland, and permanent wetland regions. Permanent snow and ice, and barren land of northern India show unimodal peak in mean LST during the month of July due to melting of seasonal snow. The interannual variability in LST is smallest during the peak months of July and August for permanent snow and ice land cover. All land covers show the smallest mean LST during the month of January and December due to the northern hemispheric winter.

3.3 Relationship between NDVI and daytime LST across India

The spatial distribution of 15-year mean monthly NDVI across India has been shown in Fig. 4a. Forest and woodland areas show rather larger magnitude of mean NDVI ranging from 0.60 to 0.80, whereas cropland and grassland regions show moderate NDVI ranging from 0.30 to 0.50. Shrublands have smaller magnitude (e.g., 0.10–0.20) of mean NDVI, and barren land areas have mean NDVI closer to zero. However, croplands and grassland areas exhibit larger seasonal variation in NDVI as compared to other land cover types.

Figure 4b illustrates the spatial distributions of correlation coefficient between simultaneous monthly NDVI and daytime LST for the study period. The regions having smallest mean daytime LST and highest elevations show positive correlation between LST and NDVI. Such positive correlation for high elevation regions were also reported by Karnieli et al. (2010). The vegetation growth over these regions is primarily controlled by energy rather than water. Other regions show negative correlation between daytime LST and NDVI. The major portions of the country are covered by cropland and thus vegetation growth largely depends on the water availability. However, the correlation is smaller for western India covered with barren land and shrubland. The northern part of northeast India shows positive correlation and southern part shows negative correlation with a north-south gradient in magnitude.

As the strength of correlations between LST and NDVI largely depends on the land cover type (Marzban et al. 2018), Fig. 5 depicts the temporal correlation coefficients between domain-mean monthly NDVI and daytime LST for different land cover types for the study period. The opposite nature of relationship between LST and NDVI can be clearly observed for the northern and western barren lands. Northern barren land shows a high positive correlation of about 0.70 between monthly LST and NDVI, whereas negative and low correlation can be seen for the western barren land. The smallest linear correlations between monthly LST and NDVI are for western desert and shrubland regions due to negligible variations in underlying soil moisture (Norouzi et al. 2015b). The cropland regions show the largest magnitude of negative correlation (~ -0.78) between LST and NDVI. The major portions of the county are covered by cropland and thus

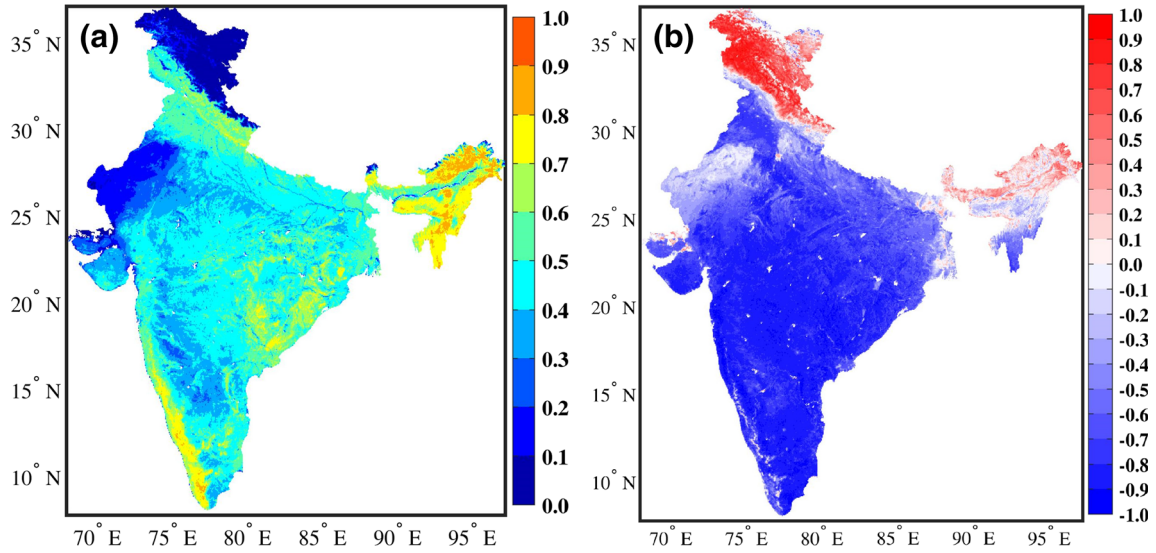

Fig. 4 Spatial distributions of **a** mean NDVI and **b** correlation coefficient between monthly NDVI and daytime LST across India for the period of 2003–2017

vegetation growth largely depends on the water availability. Forest, woodland, permanent wetland, and urban areas show a negative correlation of about 0.50 between monthly daytime LST and NDVI.

3.4 Hottest LST across India

Figure 6 shows the interannual variations of all-India mean LST for both daytime and nighttime for the period of 2003 to 2017. Daytime mean LST suggests 2009 as the warmest year followed by 2016, while 2016 was the warmest year followed by 2010 from nighttime LST estimates. If one combines daytime and nighttime LST to approximate the mean LST, 2016 would be warmest year for the country during the study period. All-India mean LST during nighttime shows a consistent increase in magnitude. The year 2016 was shown to be the warmest year at a global scale as well (Susskind et al. 2019).

The hottest or maximum LST from daily daytime MODIS data during the study period (e.g., 2003–2017) and the year of hottest LST across India are presented in Fig. 7. The magnitude of hottest LST is as high as 70 °C over the barren land of western India. The western India between 15° N and 30° N received hottest LST of 60–65 °C, and east coast and the Himalayan foothills received hottest LST of about 50 °C. Parts of western India and southern India received their hottest LST during 2016. West and east coasts of southern India received their

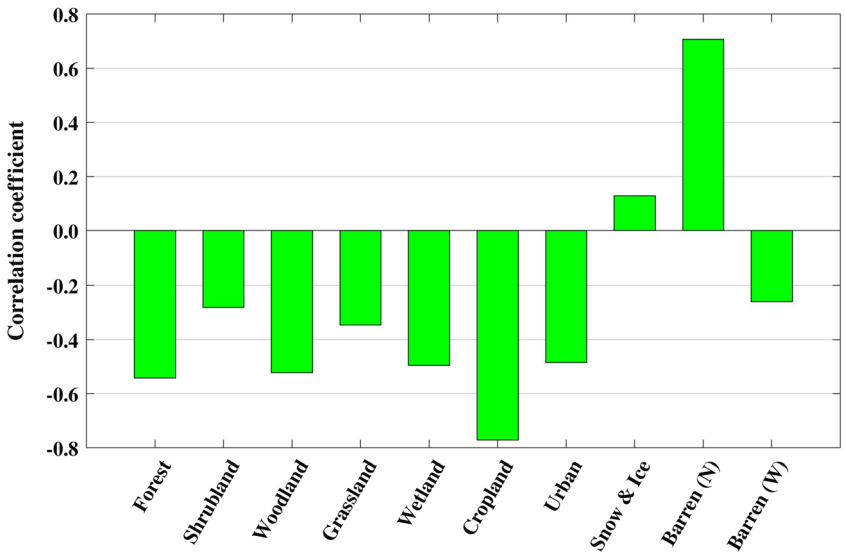

Fig. 5 Correlation coefficients for each land cover type over India after comparing domain-mean monthly NDVI and daytime LST for the period 2003–2017

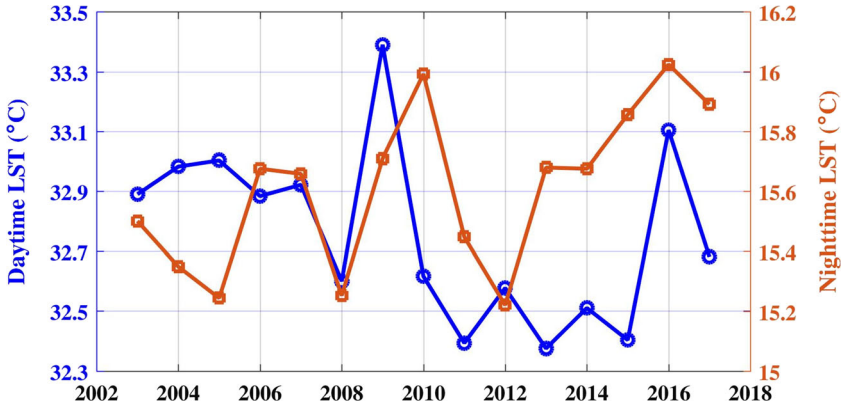

Fig. 6 Interannual variations of all-India mean LST during daytime and nighttime for the period 2003–2017

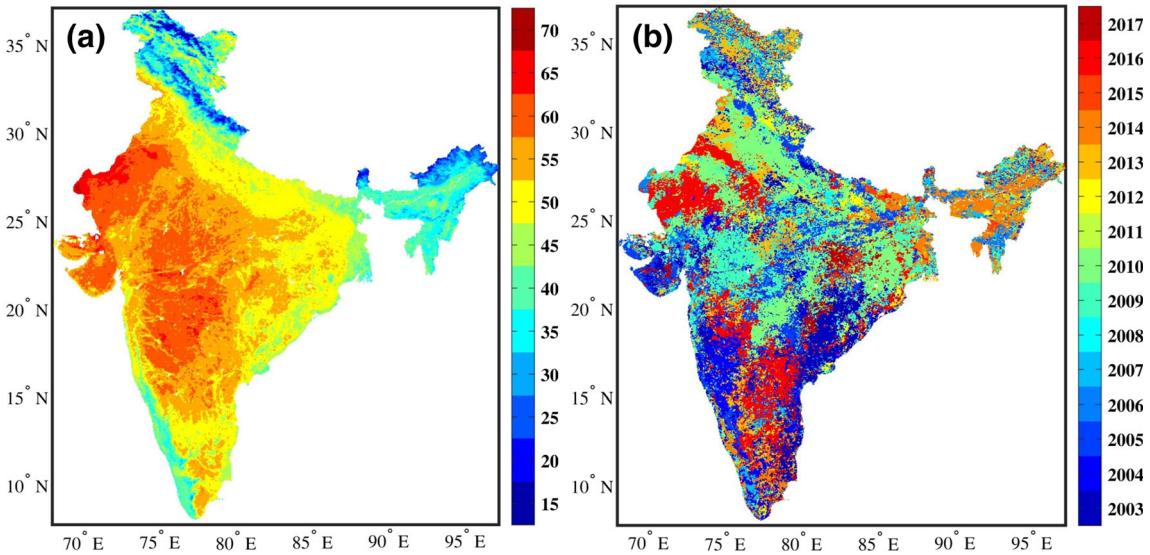

Fig. 7 Spatial distributions of **a** hottest LST (°C) between 2003 and 2017 and **b** year of hottest LST across India

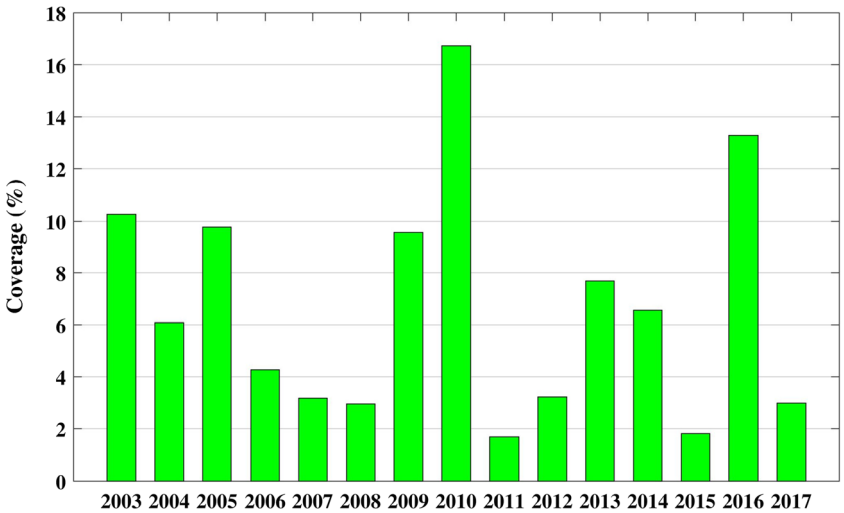

Fig. 8 Percentage coverage of Indian landmass from 15-year hottest or maximum land surface temperature

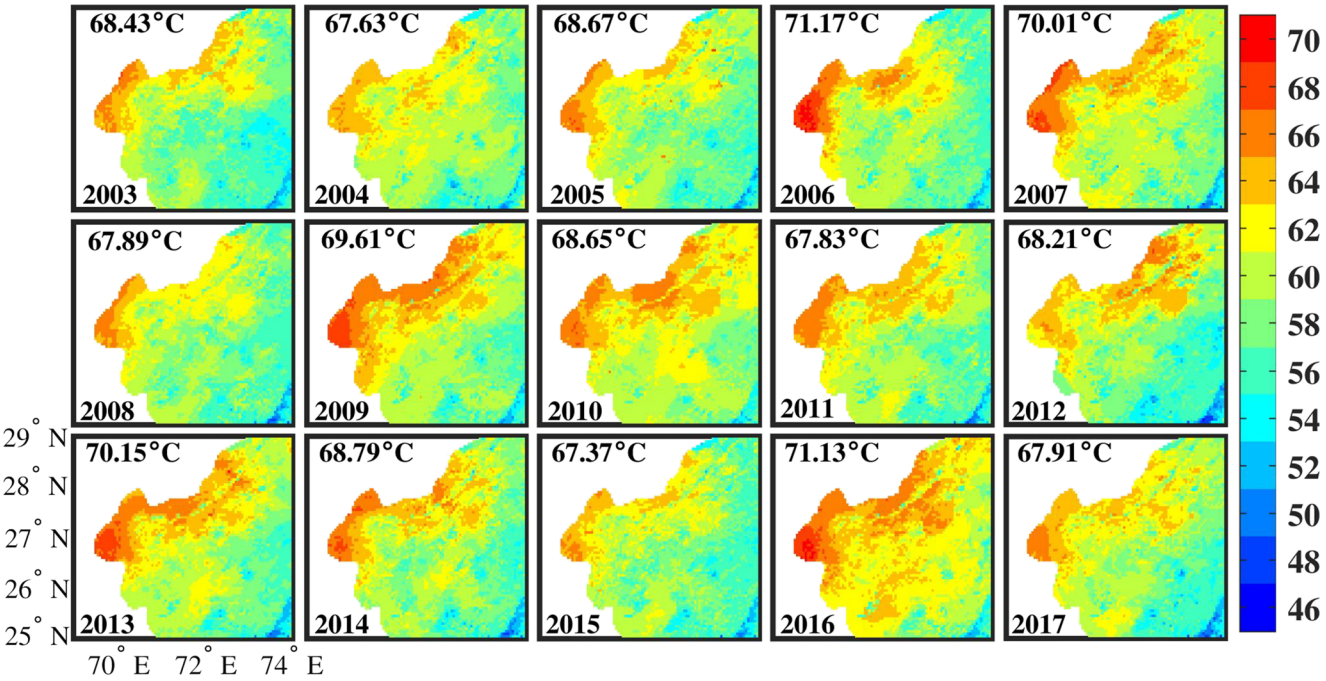

Fig. 9 Spatial distributions of annual maximum LST (°C) for each year over arid regions of northwest India for the period 2003–2017. Hottest LST within the specified region for each year is also mentioned

hottest LST during 2003, while parts of Indo-Gangetic Plain received their hottest LST during 2010. Figure 8 presents the percentage coverage of Indian landmass from hottest LST in each year of the 15-year period. About 17% of Indian landmass received its hottest LST during 2010 followed by 2016 (about 13% of Indian landmass). About 60% of the Indian landmass received its hottest LST in 5 years of 2003, 2005, 2009, 2010, and 2016.

As western India is the region getting warmest annual maximum LST across the country (e.g., Fig. 7a), spatial distributions of annual maximum LST of this region are shown in Fig. 9. The selected region is a subset of the whole Indian region and comes under the Rajasthan state. The western tip receives hottest LST of India, varying from 62 to 70 °C. This region comes under the Thar desert range and consists of barren land and shrubland (see Fig. 1b). The maximum LST recorded by the MODIS product was more than 70 °C during 4 years of 2006, 2007, 2013, and 2016. These LST values are quite larger than the reported LST of the hottest spot on the Earth, the Lut desert of the southeast Iran. Mildrexler et al. (2011) analyzed the Aqua MODIS LST Collection 5 product for 2003 to 2009, and found the maximum LST greater than 70°C during only 1 year of 2005 (70.7 °C) over the Lut desert in southeast Iran. The reason behind this discrepancy is the use of recent Collection 6 of

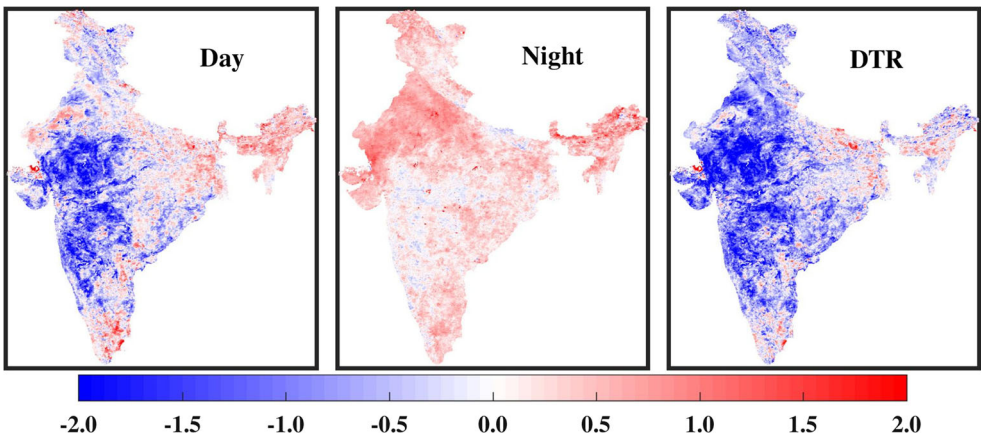

Fig. 10 Spatial distributions of linear trends in annual mean LST (°C decade^{-1}) during daytime, nighttime, and their difference between 2003 and 2017

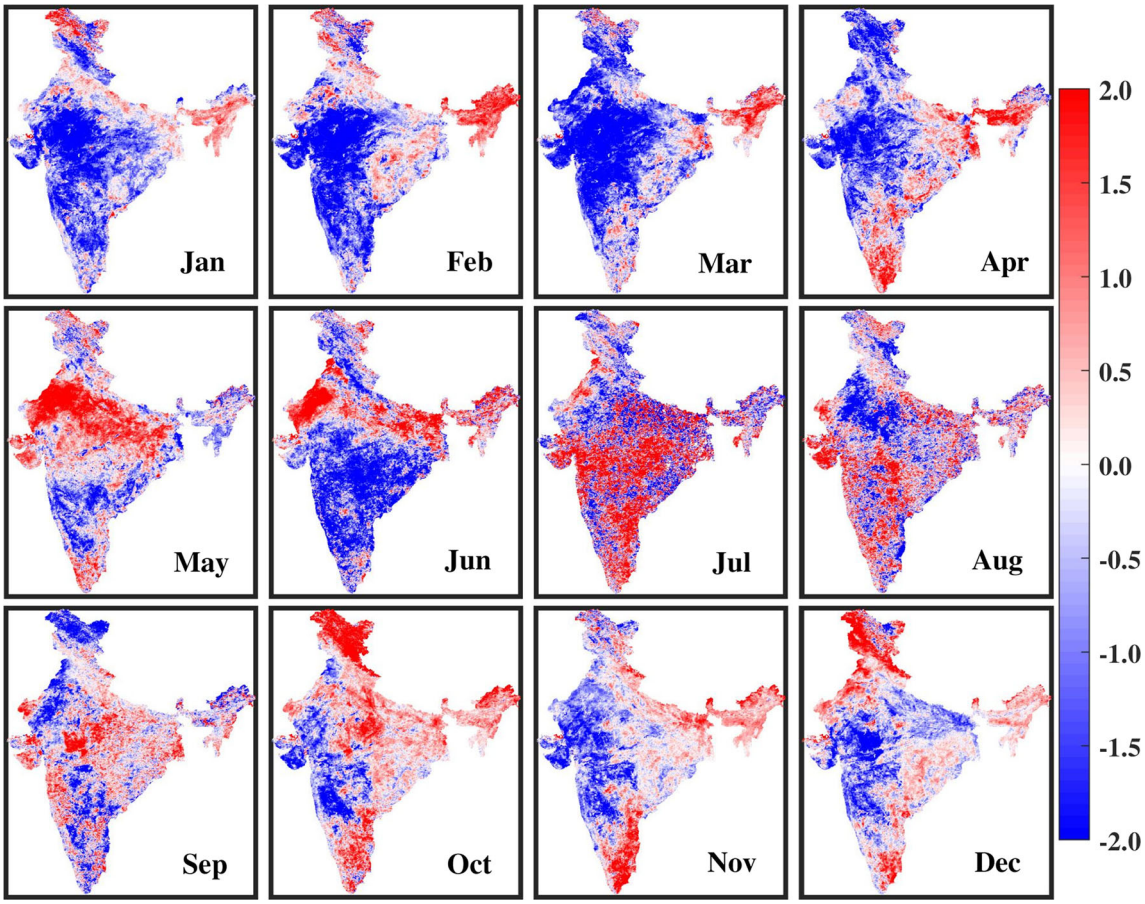

Fig. 11 Spatial distributions of linear trends in daytime LST (°C decade^{-1}) for each month between 2003 and 2017

MODIS LST product in this study, which provides 2–4 °C higher LST than Collection 5 estimates over the arid regions (Prakash et al. 2018). The evaluation of both Collections of LST showed notable improvement in Collection 6 estimates over Collection 5 estimates due to several refinements (Wan 2014; Duan et al. 2019). The largest area of this region (i.e., 23.42% area of the selected region) received annual maximum LST of greater than 65 °C during 2016 followed by 2009 (20.13% area of the selected region). The smallest land coverage of about 3% of the specified region by annual maximum LST of more than 65 °C was observed during 2004 and 2015. Overall, the annual maximum LST did not show any systematic change over this region during the study period.

3.5 Changes in LST between 2003 and 2017 across India

In this section, changes in LST across India are investigated for the 15-year period. Figure 10 shows the spatial distributions of linear trends in mean annual LST for daytime, nighttime, and DTR. The southern tip and northeast India show an increase in daytime LST, whereas western and southwestern parts of the country exhibit a decline. The nighttime LST shows an increasing trend over most parts of the country. The magnitude of increase in nighttime LST is larger (~2 °C decade^{-1}) over the western and northeast India. As nighttime LST is increasing at a faster rate than daytime LST, most parts of the country show a decrease in annual DTR. These results are similar as the linear trends of DTR in near-surface air temperature over India (Vinnarasi et al. 2017).

In addition, the short-term changes in daytime and nighttime LST have been investigated for each month separately. Figures 11 and 12 show the spatial distributions of linear trends in daytime and nighttime LST across the country, respectively. The decline in daytime LST is prominent over the western and southwestern India during January to March, whereas increase in LST over the western India and over the Himalayan foothills region is pronounced during May and June. Nighttime LST also shows a distinctive trend during each month. The increase in nighttime LST over the northern parts is largest during the May, June, and October months.

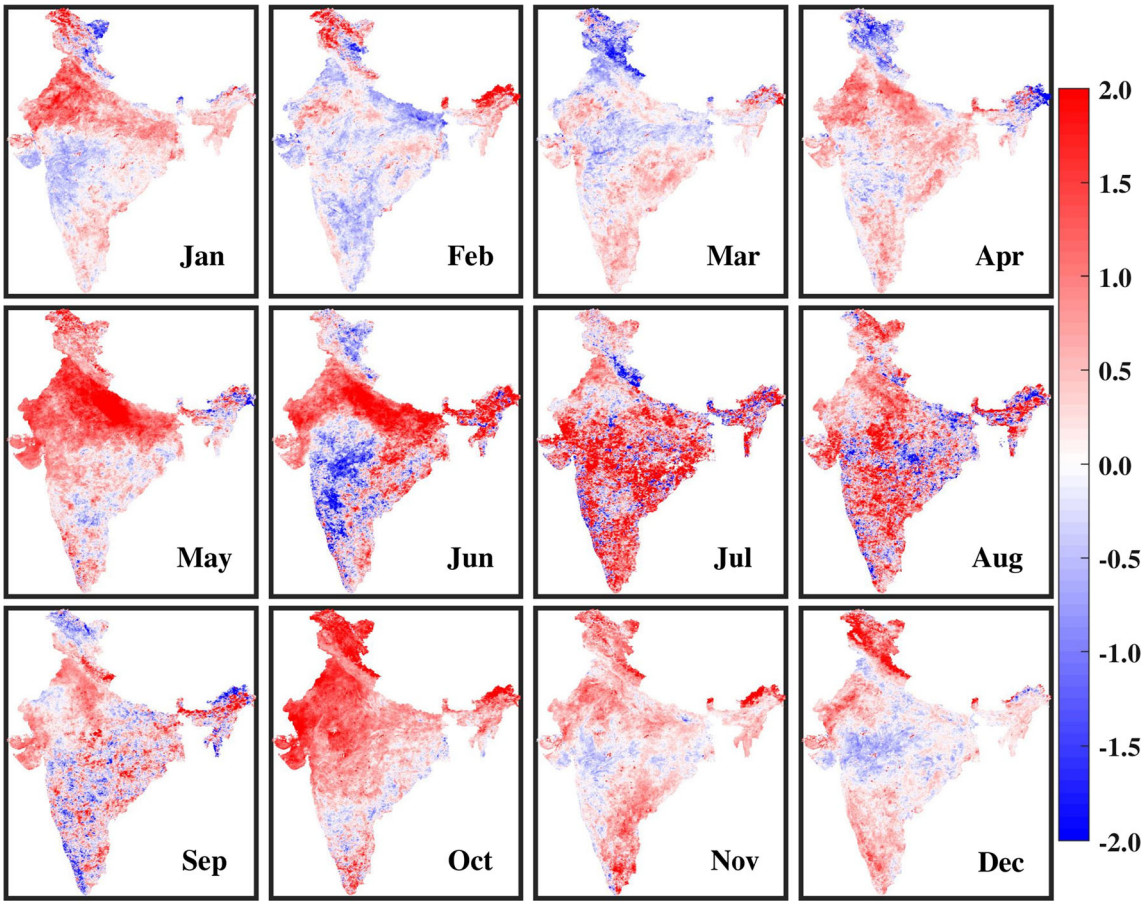

Fig. 12 Spatial distributions of linear trends in nighttime LST (°C decade^{-1}) for each month between 2003 and 2017

It is worthy to mention here that these trend analyses results are based on 15 years of MODIS datasets and are not sufficient for a robust climatic trend analysis. However, these results provide a preliminary guidance to recent changes in LST across India for several environmental applications. Furthermore, MODIS provides LST for clear-sky conditions only. Figure 13 illustrates the all-India mean cloud cover from the Aqua MODIS for the period of 2003–2017. It clearly indicates that 70–90% area of the country used to be covered with clouds during the southwest monsoon season (e.g., June–September). Therefore, mean LST estimates and its trend over India during these months might have larger uncertainty.

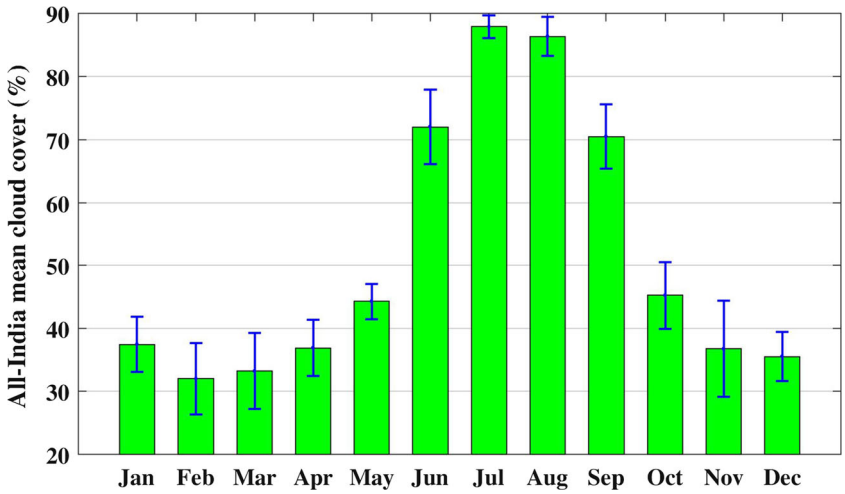

Fig. 13 Monthly variations in all-India mean cloud cover from Aqua measurements for the period 2003–2017. The error bars represent the interannual variability

4 Conclusion

This study investigated the mean LST and its variability across India exclusively from the Aqua MODIS data at 0.05° spatial resolution for the period of 2003 to 2017. The mean features of LST averaged over the country were not essentially the same as the mean features of near-surface air temperature. In general, all land cover types exhibited bimodal peaks in mean monthly daytime LST except for permanent snow and ice, and cold desert areas. Permanent snow and ice, and barren land of northern India showed unimodal peak in mean LST during the month of July. The linear relationship between simultaneous monthly mean daytime LST and NDVI were also assessed for different land cover types across the country. The high-altitude regions of northern India showed the smallest mean daytime LST and anomalous positive correlation with NDVI at monthly scale. The monthly domain-mean daytime LST of cropland regions were highly negatively correlated with NDVI as compared to other land cover types. The analysis of daytime LST indicated that about 17% of Indian landmass received its hottest LST during 2010 followed by 2016. Additionally, the annual maximum LST recorded by the MODIS product was greater than 70 °C for the western India during 2006, 2007, 2013, and 2016. The spatial coverage of annual maximum LST greater than 65 °C over this arid region was largest during 2016 followed by 2009. The linear trend analysis for the 15-year period showed an increase in nighttime LST over most parts of the country, while daytime LST showed a decline over the western and southwestern India. However, both daytime and nighttime LST exhibited distinctive features of linear trends for each month.

There are two limitations of this study. First, 15-year data is not sufficient for a conclusive climatic trend analysis. Secondly, MODIS essentially provides LST estimates during clear-sky conditions only and India gets substantial cloud cover (~ 70–90%) during the southwest monsoon season. There is a need to develop a suitable technique to estimate global LST for all-weather conditions by the synergistic use of infrared and microwave measurements. The evaluation of MODIS LST products with ground-based observations showed reasonably good agreement over the selected global validation sites (Wan 2014; Duan et al. 2019), but the errors in the satellite-based daytime LST estimates were shown to be rather larger over several stations of the North America (Prakash et al. 2019). The lack of ground-based observations of LST at a global scale limits the comprehensive evaluation of satellite-based LST estimates. Needless to say that the augmentation of ground-based observations of LST would certainly improve the accuracy of satellite-based LST estimates at global and regional scales.

Acknowledgment The authors would like to thank the editor and anonymous reviewer for their constructive comments. The MODIS data products were obtained from the online Data Pool, courtesy of the NASA Land Processes Distributed Active Archive Center (LP DAAC), USGS/Earth Resources Observation and Science (EROS) Center, Sioux Falls, South Dakota, https://lpdaac.usgs.gov/data_access/data_pool.

References

Deilami K, Kamruzzaman M, Liu Y (2018) Urban heat island effect: a systematic review of spatio-temporal factors, data, methods, and mitigation measures. Int J Appl Earth Obs Geoinf 67:30–42. https://doi.org/10.1016/j.jag.2017.12.009

Didan K (2015) MYD13C2 MODIS/Aqua Vegetation Indices Monthly L3 Global 0.05Deg CMG V006. NASA EOSDIS LP DAAC. https://doi.org/10.5067/MODIS/MYD13C2.006

Didari S, Norouzi H, Zand-Parsa S, Khanbilvardi R (2017) Estimation of daily minimum land surface air temperature using MODIS data in southern Iran. Theor Appl Climatol 130:1149–1161. https://doi.org/10.1007/s00704-016-1945-0

Duan S-B, Li Z-L, Li H, Gottsche F-M, Wu H, Zhao W, Leng P, Zhang X, Coll C (2019) Validation of Collection 6 MODIS land surface temperature product using in situ measurements. Remote Sens Environ 225:16–29. https://doi.org/10.1016/j.rse.2019.02.020

Friedl M, Sulla-Menashe D (2015) MCD12C1 MODIS/Terra+Aqua Land cover type yearly L3 global 0.05Deg CMG V006. NASA EOSDIS Land Processes DAAC.https://doi.org/10.5067/MODIS/MCD12C1.006.

Gesch DB, Larson KS (1996) Techniques for development of global 1-kilometer digital elevation models. In *Pecora Thirteen, Human Interactions with the Environment – Perspectives from Space*, Sioux Falls, South Dakota.

Hao Z, AghaKouchak A, Phillips TJ (2013) Changes in concurrent monthly precipitation and temperature extremes. Environ Res Lett 8:034014. https://doi.org/10.1088/1748-9326/8/3/034014

Justice CO, Vermote E, Townshend JRG, Defries R, Roy DP, Hall DK, Salomonson VV, Privette JL, Riggs G, Strahler A, Lucht W, Myneni RB, Lewis P, Barnsley MJ (1998) The Moderate Resolution Imaging Spectroradiometer (MODIS): Land remote sensing for global change research. IEEE Trans Geosci Remote Sens 36:1228–1249

Karnieli A, Agam N, Pinker RT, Anderson M, Imhoff ML, Gutman GG, Panov N, Goldberg A (2010) Use of NDVI and land surface temperature for drought assessment: Merits and limitations. J Clim 23:618–633. https://doi.org/10.1175/2009JCLI2900.1

Khandan R, Gholamnia M, Duan S-B, Ghadimi M, Alavipanah SK (2018) Characterization of maximum land surface temperatures in 16 years from MODIS in Iran. Environ Earth Sci 77:450–411. https://doi.org/10.1007/s12665-018-7623-z

Li Z-L, Tang B-H, Wu H, Ren H, Yan G, Wan Z, Trigo IF, Sobrino JA (2013) Satellite-derived land surface temperature: current status and perspectives. Remote Sens Environ 131:14–37. https://doi.org/10.1016/j.rse.2012.12.008

Li Y, Zhao M, Mildrexler DJ, Motesharrei S, Mu Q, Kalnay E, Zhao F, Li S, Wang K (2016) Potential and actual impacts of deforestation and afforestation on land surface temperature. J Geophys Res - Atmos 121:14372–14386. https://doi.org/10.1002/2016JD024969

Marzban F, Sodoudi S, Preusker R (2018) The influence of land-cover type on the relationship between NDVI-LST and LST-T_{air}. Int J Remote Sens 39:1377–1398. https://doi.org/10.1080/01431161.2017.1402386

Mathew A, Khandelwal S, Kaul N (2017) Investigating spatial and seasonal variations of urban heat island effect over Jaipur city and its relationship with vegetation, urbanization and elevation

parameters. Sustain Cities Soc 35:157–177. https://doi.org/10.1016/j.scs.2017.07.013

Mildrexler DJ, Zhao M, Running SW (2011) Satellite finds highest land skin temperatures on Earth. Bull Amer Meteor Soc 92:855–860. https://doi.org/10.1175/2011BAMS3067.1

Mildrexler DJ, Zhao M, Cohen WB, Running SW, Song XP, Jones MO (2018) Thermal anomalies detect critical global land surface changes. J Appl Meteorol Climatol 57:391–411. https://doi.org/10.1175/JAMC-D-17-0093.1

Norouzi H, Temimi M, AghaKouchak A, Azarderakhsh M, Khanbilvardi R, Shields G, Tesfagiorgis K (2015a) Inferring land surface parameters from the diurnal variability of microwave and infrared temperatures. Phys Chem Earth 83-84:28–35. https://doi.org/10.1016/j.pce.2015.01.007

Norouzi H, Temimi M, Prigent C, Turk J, Khanbilvardi R, Tian Y, Furuzawa FA, Masunaga H (2015b) Assessment of the consistency among global microwave land surface emissivity products. Atmos Meas Tech 8:197–1205. https://doi.org/10.5194/amt-8-1197-2015

Parida BR, Oinam B, Patel NR, Sharma N, Kandwal R, Hazarika MK (2008) Land surface temperature variation in relation to vegetation type using MODIS satellite data in Gujarat state of India. Int J Remote Sens 29:4219–4235. https://doi.org/10.1080/01431160701871096

Parkinson CL (2013) Summarizing the first ten years of NASA's Aqua mission. IEEE J Sel Top Appl Earth Obs Remote Sens 6:1179–1188. https://doi.org/10.1109/JSTARS.2013.2239608

Patel S, Joshi JP, Bhatt B (2017) An assessment of spatio-temporal variability of land surface temperature using MODIS: a study of Gujarat state, India. Geogr Compass 11:e12312. https://doi.org/10.1111/gec3.12312

Phan TN, Kappas M (2018) Application of MODIS land surface temperature data: a systematic literature review and analysis. J Appl Remote Sens 12:041501. https://doi.org/10.1117/1.JRS.12.041501

Platnick S, Hubanks P, Meyer K, King MD (2015) MODIS Atmosphere L3 monthly product (08_L3). NASA MODIS adaptive processing system, Goddard Space Flight Center, USA. https://doi.org/10.5067/MODIS/MYD08_M3.006.

Prakash S (2018) Capabilities of satellite-derived datasets to detect consecutive Indian monsoon droughts of 2014 and 2015. Curr Sci 114:2362–2368. https://doi.org/10.18520/cs/v114/i11/2362-2368

Prakash S, Norouzi H, Azarderakhsh M, Blake R, Tesfagiorgis K (2016) Global land surface emissivity estimation from AMSR2 observations. IEEE Geosci Remote Sens Lett 13:1270–1274. https://doi.org/10.1109/LGRS.2016.2581140

Prakash S, Norouzi H, Azarderakhsh M, Blake R, Khanbilvardi R (2017) Potential of satellite-based land emissivity estimates for the detection of high-latitude freeze and thaw states. Geophys Res Lett 44:2336–2342. https://doi.org/10.1002/2017GL072560

Prakash S, Norouzi H, Azarderakhsh M, Blake R, Prigent C, Khanbilvardi R (2018) Estimation of consistent global microwave land surface emissivity from AMSR-E and AMSR2 observations. J Appl Meteorol Climatol 57:907–919. https://doi.org/10.1175/JAMC-D-17-0213.1

Prakash S, Shati F, Norouzi H, Blake R (2019) Observed differences between near-surface air and skin temperatures using satellite and ground-based data. Theor Appl Climatol 137:587–600. https://doi.org/10.1007/s00704-018-2623-1

Prigent C, Jimenez C, Aires F (2016) Toward "all-weather", long record, and real-time land surface temperature retrievals from microwave satellite observations. J Geophys Res - Atmos 121:5699–5717. https://doi.org/10.1002/2015JD024402

Roy PS et al (2015) Development of decadal (1985-1995-2005) land use and land cover database for India. Remote Sens 7:2401–2430. https://doi.org/10.3390/rs70302401

Schmidt GA, Shindell DT, Tsigaridis K (2014) Reconciling warming trends. Nat Geosci 7:158–160. https://doi.org/10.1038/ngeo2105

Sharifnezhadazizi Z, Norouzi H, Prakash S, Beale C, Khanbilvardi R (2019) A global analysis of land surface temperature diurnal cycle using MODIS observations. J Appl Meteorol Climatol 58:1279–1291. https://doi.org/10.1175/JAMC-D-18-0256.1

Shati F, Prakash S, Norouzi H, Blake R (2018) Assessment of differences between near-surface air and soil temperatures for reliable detection of high-latitude freeze and thaw states. Cold Reg Sci Technol 145:86–92. https://doi.org/10.1016/j.coldregions.2017.10.007

Singh R, Singh C, Ojha SP, Kumar AS, Kishtawal CM, Kiran Kumar AS (2016) Land surface temperature from INSAT-3D imager data: Retrieval and assimilation in NWP model. J Geophys Res - Atmos 121:6909–6926. https://doi.org/10.1002/2016JD024752

Sulla-Menashe D, Gray JM, Abercrombie SP, Friedl MA (2019) Hierarchical mapping of annual global land cover 2001 to present: The MODIS Collection 6 land cover product. Remote Sens Environ 222:183–194. https://doi.org/10.1016/j.rse.2018.12.013

Susskind J, Schmidt GA, Lee JN, Iredell L (2019) Recent global warming as confirmed by AIRS. Environ Res Lett 14:044030. https://doi.org/10.1088/1748-9326/aafd4e

Turco M, Palazzi E, Hardenberg J, Provenzale A (2015) Observed climate change hotspots. Geophys Res Lett 42:3521–3528. https://doi.org/10.1002/2015GL063891

Vinnarasi R, Dhanya CT, Chakravorthy A, AghaKouchak A (2017) Unravelling diurnal asymmetry of surface temperature in different climate zones. Sci Rep 7:7350. https://doi.org/10.1038/s41598-017-07627-5

Wan Z (2014) New refinements and validation of the collection-6 MODIS land-surface temperature/emissivity product. Remote Sens Environ 140:36–45. https://doi.org/10.1016/j.rse.2013.08.027

Wan Z, Hook S, Hulley G (2015) MYD11C1 MODIS/Aqua Land Surface Temperature/Emissivity Daily L3 Global 0.05Deg CMG V006. NASA EOSDIS LP DAAC. https://doi.org/10.5067/MODIS/MYD11C1.006.

Wei N, Zhou L, Dai Y, Xia G, Hua W (2017) Observational evidence for desert amplification using multiple satellite datasets. Sci Rep 7:2043. https://doi.org/10.1038/s41598-017-02064-w

Zhao W, He J, Wu Y, Xiong D, Wen F, Li A (2019) An analysis of land surface temperature trends in the central Himalayan region based on MODIS products. Remote Sens 11:900. https://doi.org/10.3390/rs11080900